Silicon (2023) 15:5307–5315
https://doi.org/10.1007/s12633-023-02430-6

RESEARCH

Numerical Study on the Effect of Water-cooling Jacket Radius on Czochralski Silicon

Wenjia Su[1] · Jiaqi Li[1] · Jiulong Li[2] · Zhicheng Guan[1] · Zhen Zhang[1]

Received: 12 February 2023 / Accepted: 22 March 2023 / Published online: 1 April 2023
© Springer Nature B.V. 2023

Abstract
In order to create a suitable temperature environment in the cooling process of Czochralski silicon (Cz-Si), a water-cooling jacket is usually set, which can improve the crystal temperature gradient and the crystal cooling rate. In this paper, a 2D global quasi-steady axisymmetric model is established to simulate the effects of water-cooling jacket radius of the melt flow and heat transfer, solid–liquid (S-L) interface shape and crystal thermal stress during the silicon crystal growth process. The results show that changing the radius of the water-cooling jacket has less effect on the melt flow, but more significant effect on the crystal heat transfer. The smaller the radius of the water-cooling jacket, the higher the argon flow rate nearby, the better the cooling effect, it will reduce the convexity of the S-L interface and the thermal stress. According to the calculation results, compared with $\Delta R = 35$ mm and 55 mm, the crystal pulling rate of $\Delta R = 15$ mm can be increased by 27.1% and 36.1% respectively.

Keywords Computer simulation · Heat transfer · Fluid flow · Czochralski method · Silicon

1 Introduction

Monocrystalline silicon is the primary material of solar photovoltaic panels. The Cz method was proposed as early as 1918 [1]. It is now widely used in the solar photovoltaic and semiconductor industries [2]. The standard Cz method takes a long time to grow crystals. The current sector aims to improve productivity and economic efficiency by improving the growth rate of crystals [3]. It is necessary to raise the axial temperature gradient of the crystal to increase the crystal growth rate [4]. Huang et al. [5] verified the relationship between the crystal temperature gradient and the heat balance equation near the S-L interface. They found that increasing the crystal growth rate will increase the temperature gradient and release more solidification latent heat, causing excessive thermal stress, which makes the crystal highly prone to dislocation [6].

✉ Wenjia Su
wjsu@ujs.edu.cn

[1] School of Energy and Power Engineering, Jiangsu University, Zhenjiang 212013, Jiangsu, China

[2] The Institute of Technological Sciences, Wuhan University, Wuhan 430072, Hubei, China

In Czochralski monocrystalline silicon growth, a heat shield is usually set to block the thermal radiation from the high-temperature heater and crucible to the crystal, reducing the radial temperature gradient and creating a good cooling environment [7]. The heat shield in the furnace affects the argon flow rate, crystal temperature gradient, S-L interface shape, thermal stress, and crystal growth rate. Optimizing the structure of the heat shield can control the distribution of the thermal and flow fields in the furnace, affecting the shape of the S-L interface and the oxygen impurity content of the melt, thus improving the crystal quality [8–11].

In addition to the heat shield, some scholars added a water-cooling jacket to the periphery of the crystal. The constant temperature water-cooling jacket can enhance the crystal cooling rate and help to release the latent heat at the S-L interface. Friedrich et al. [12] found that the addition of an active crystal cooler device can increase the limited growth rate of the crystal to 2 mm/min without twisting. Jeon et al. [3] set up two new cooling systems above the heat shield. The simulation results showed that the crystal growth rate increased by more than 18.1%, and the thermal stress inside the crystal decreased by 15%. Sim et al. [13] improved the crystal cooling rate and S-L interface shape by using the water-cooling jacket of different materials and changing the distance between the heat shield and the melt free surface,

thereby increasing the critical pulling rate. Zhao et al. [14] increased the crystal growth rate by 20% by setting the water-cooling jacket and upgrading the heat shield structure. However, Qi et al. [15] found that the water-cooling jacket increases the oxygen content at the S-L interface. Most of the research on water-cooling jackets improves the crystal growth rate by improving their shape and material, which is difficult and costly.

In this contribution, numerical modeling was used to investigate the melt flow and heat transport during Cz-Si growth with an 8.5-inch diameter from an initial charge weight of 400 kg in a crucible with a 28-inch diameter. This work focuses on identifying the possible pulling rates for different hot zones.

2 Numerical modeling

A 2D quasi-steady heat transfer and numerical flow model of Cz-Si was established in ANSYS Fluent by referring to the industrial furnace. An inverted conical, cylindrical water-cooling jacket was arranged between the heat shield and the crystal, as shown in Fig. 1a. The jacket temperature was 300 K, the rotation rate of the crystal and crucible was 9.5 rpm and -9 rpm, respectively, and the furnace pressure was 14 Torr. The radius difference between the crystal and the jacket was considered ΔR; three values were compared (ΔR = 15 mm, 35 mm and 55 mm). The distance between the heat shield and the jacket remained constant; that is, the radius of the heat shield changed with the jacket. The flow velocity of the argon inlet was determined by the industrial process parameters. The argon outlet adopted the natural outflow boundary condition.

According to industrial production and numerical simulation, the crystal pulling rate of 1.7 mm/min is high enough with fewer defect. Increasing the pulling rate can lead to crystal fracture, dislocations and crystal twisting [12]. Therefore, the crystal pulling rate is set as 1.7 mm/min in this contribution. Considering the latent heat release, it is assumed that the crystal growth rate is equal to the pulling rate. Based on this, the radius of the water-cooling jacket is changed to improve the hot zone, and its influence on the crystal pulling rate is studied when the crystal growth height is 1500 mm.

Figure 1b shows the grids of the furnace. For the Cz-Si furnace, solid parts and silicon regions are axisymmetric, and the results of 2D simulation and 3D simulation are similar [16]; the 2D axisymmetric model can be used for the geometric furnace modeling. A structural/unstructured hybrid grid and size function were used to refine the boundary grids. Additionally, the grids of the melt and crystal were densified to capture the changes in physical quantities more accurately. Table 1 shows the physical parameters of the materials used.

To simplify the calculation, the following assumptions are adopted [17]: all radiation surfaces are diffuse gray surfaces, the melt is a Newtonian fluid and is incompressible, the Boussinesq hypothesis is applied when there is thermal buoyancy of the melt, argon is an incompressible gas and meets the ideal gas equation, the Cz-Si growth process is regarded as a quasi-steady process. The governing equation is [18]:

$$\nabla \bullet \vec{u} = 0 \tag{1}$$

$$\nabla \bullet \left(\rho \vec{u}\vec{u}\right) = -\nabla p + \nabla \bullet \left[\mu_{eff}\left(\nabla \vec{u} + \nabla \vec{u}^{T}\right)\right] - \rho \vec{g} \beta_T \left(T - T_{ref}\right) \tag{2}$$

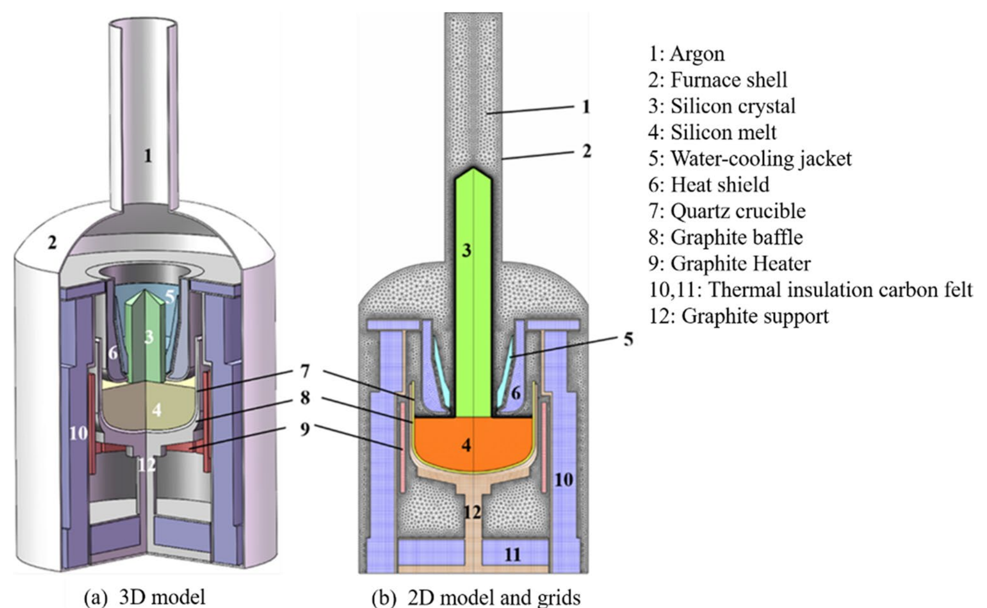

Fig. 1 Schematic diagram and calculation mesh of industrial Cz furnace

Table 1 Physical properties of materials

Material	Density/kg·m^{-3}	Specific heat capacity/ J·kg^{-1}·K^{-1}	Thermal conductivity /W·m^{-1}·K^{-1}	Emissivity ——
Si(crystal)	2300	950	22	0.318
Quartz crucible	1930	1059	4	0.6
Carbon felt	2101	-317 + 4.03 T-0.00024T^2 + 5.0 × 10^{7}T^3	0.5	0.45
Steel	7900	477	15	0.22
Graphite	1830	2019	90	0.8
Si(melt)	2530	1040	57	0.318
Argon	——	520.64	0.2373	——

$$\nabla \bullet = \left(\rho C_p \vec{u} T\right) = \nabla \bullet \left(\lambda_{eff} \nabla T\right) \tag{3}$$

$$\nabla \bullet (\lambda \nabla T) + S_Q = 0 \tag{4}$$

where, $\vec{u}$ is the velocity, ρ is the density, μ_{eff} is the effective dynamic viscosity, p is the pressure, T is the temperature, T_{ref} is the reference temperature, β_T is the thermal expansion coefficient, $\vec{g}$ the gravitational acceleration vector, C_p is the thermal capacity, λ_{eff} is the effective thermal conductivity, and S_Q is the thermal emissivity per unit volume.

The latent heat released at the S-L interface and the crystal growth rate satisfy the heat balance equation:

$$\rho \Delta H v_g = \left(\lambda \frac{\partial T}{\partial n}\right)_{\text{crystal}} - \left(\lambda \frac{\partial T}{\partial n}\right)_{\text{melt}} \tag{5}$$

where, ΔH is the latent heat of crystallization, v_g is the pulling rate, λ is the thermal conductivity, $\frac{\partial T}{\partial n}$ is the temperature gradient perpendicular to the S-L interface.

Considering the shear force of argon and Marangoni effect, the boundary conditions are as fosllows:

$$v_{\tau gas} = v_{\tau melt} = 0 \tag{6}$$

$$\mu_{melt} \frac{\partial v_{tmelt}}{\partial n} = \left(\mu_{gas} + \mu_{melt}\right) \frac{\partial v_{\tau gas}}{\partial n} + \frac{\partial \sigma}{\partial T} \frac{\partial T}{\partial \tau} \tag{7}$$

where, $\frac{\partial \sigma}{\partial T}$ is the surface tension temperature coefficient, $v_{\tau melt}$ 和 $v_{\tau gas}$ is the tangential velocity of gas and melt, μ_{melt} 和 μ_{gas} is the dynamic viscosity coefficient of gas and melt.

The thermal stress is expressed by Von Mises stress, and the calculation formula is:

$$\sigma_{von} = \frac{\sqrt{\left(\sigma_{rr} - \sigma_{zz}\right)^2 + \left(\sigma_{\phi\phi} - \sigma_{rr}\right)^2 + \left(\sigma_{\phi\phi} - \sigma_{zz}\right)^2 + 6\left(\sigma_{rz}{}^2 + \sigma_{r\phi}{}^2 + \sigma_{\phi z}{}^2\right)}}{2} \tag{8}$$

3 Results and discussion

3.1 Effect of water-cooling jacket on argon flow

Changing the jacket radius will affect the argon flow, thus affecting the convection heat transfer between the argon and crystal. A smaller ΔR means the flow path between the crystal and the jacket is narrower. As shown in Fig. 2, the argon flow velocity above the crystal surface and the melt free surface can reach 8 m/s and 20 m/s, respectively, when ΔR = 15 mm. The jacket being close to the crystal can enhance the convection heat transfer and improve the cooling effect in the crystal. However, during actual growth, the high-speed argon scours the crystal surface and meniscus, which may impact the crystal surface, causing the crystal rod to shake and the meniscus shape to deform, thus affecting the normal growth of the crystal.

3.2 Effect of water-cooling jacket on melt temperature and flow

The melt flow is complex due to the combined effect of various forces. Figure 3 shows the temperature field and flow field distributions of silicon melt with different radii of the water-cooling jacket. It can be seen that three obvious vortices are formed in the melt, as well as other small, complex, irregular flows. Among them, the large vortex cell near the side wall of the crucible is the thermal buoyancy vortex caused by uneven temperature. Due to crystal and crucible rotation, the Taylor-Proudman vortex is formed below the S-L interface. The vortex cell in the middle is a secondary convection

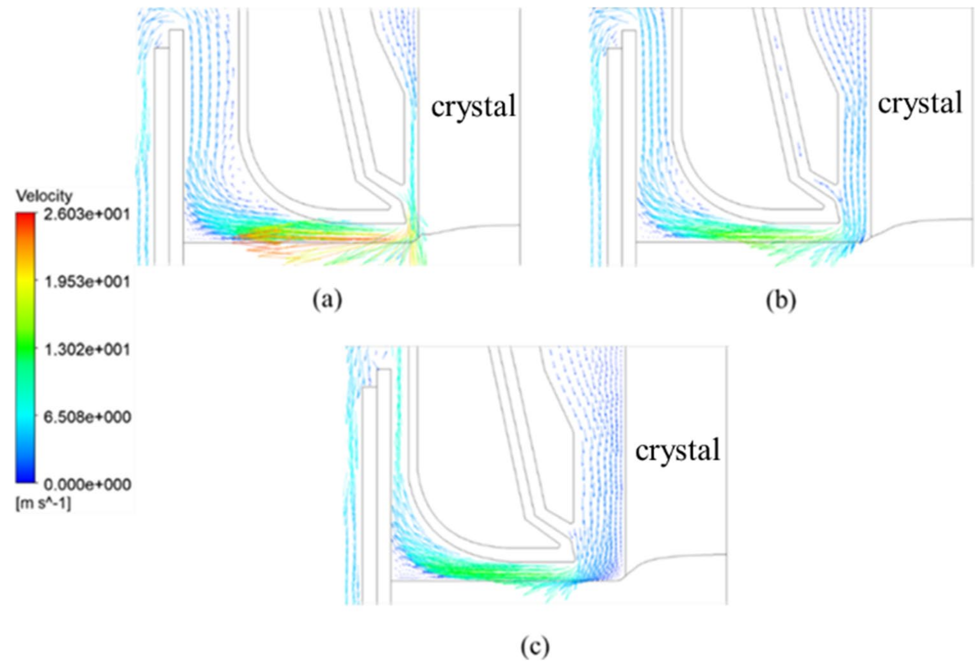

Fig. 2 The argon flow rate when (**a**) ΔR = 15 mm, (**b**) ΔR = 35 mm, (**c**) ΔR = 55 mm

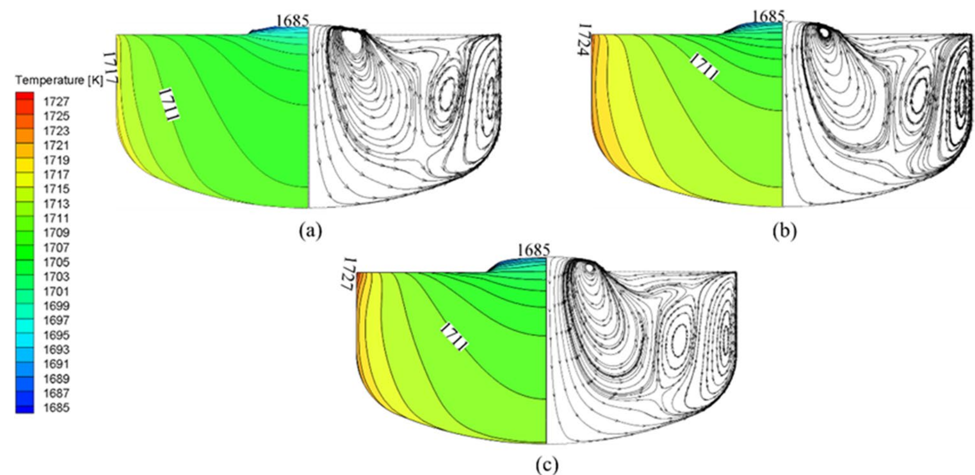

Fig. 3 The temperature field (left) and flow field (right) distributions of the melt when (**a**) ΔR = 15 mm, (**b**) ΔR = 35 mm, (**c**) ΔR = 55 mm

vortex created by the combined action of thermal buoyancy vortex, Taylor-Proudman vortex, argon shear force, and thermal capillary convection generated by surface tension, and it is a weak flow. The melt flow of the three cases is similar, but the melt temperature on the crucible side wall increases gradually with the increase of ΔR. The melt radiative heat transfer area magnifies with ΔR increases; to maintain the triple point temperature at 1685 K, the heat transferred by the heater increases. At the same time, when ΔR = 55 mm, the heat shield is closer to the crucible side wall where the melt surface radiative heat transfer is blocked, and the heat dissipation is reduced, causing the crucible side wall temperature to rise. When ΔR is 15 mm, 35 mm and 55 mm, the maximum temperature difference of the silicon melt is 32 K, 39 K, and 42 K, respectively. However, the decomposition rate of the quartz crucible increases as the melt temperature rises, causing more oxygen impurities to dissolve into the melt. Too much oxygen impurities at the S-L interface will lead to defects and dislocations in the crystal, increasing resistivity and affecting the electrical properties. Therefore, the change of the jacket radius has little effect on melt flow, but it will affect the melt thermal field distribution.

3.3 Effect of water-cooling jacket on heat flux

The actual radiative heat transfer between radiant surfaces is determined by Stephen Boltzmann's law:

$$Q_{rad} = \varepsilon \bullet \sigma \bullet S_1 \bullet X_{S_1 S_2} \bullet \left(T_1^4 - T_2^4\right) \quad (9)$$

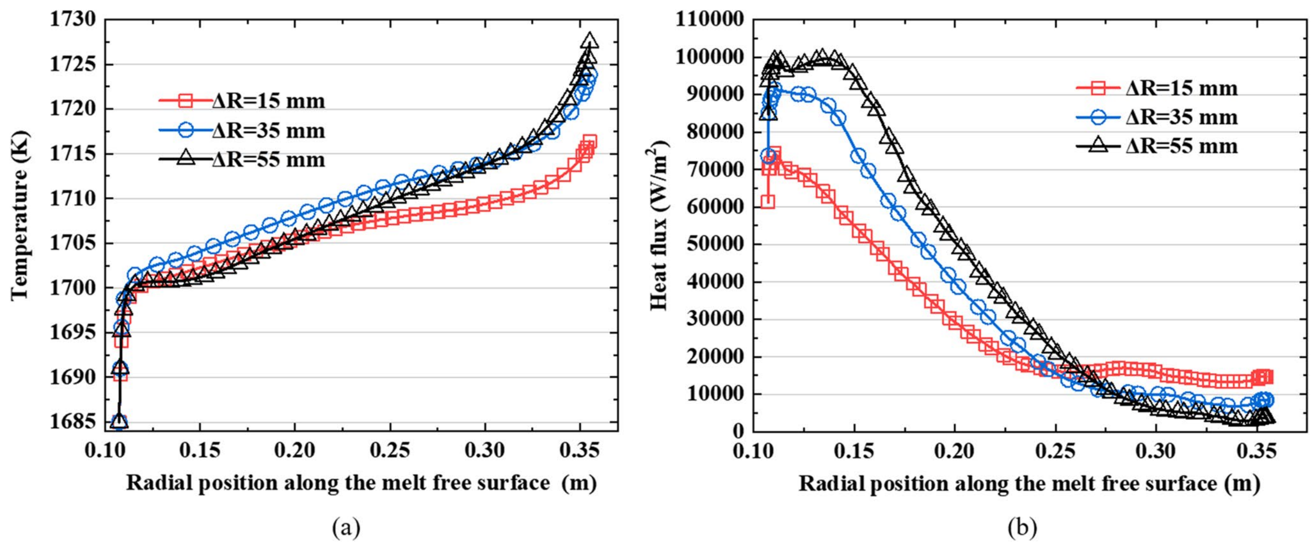

Fig. 4 **a** Temperature and **b** heat flux distributions along the melt free surface

where, ε is the radiative emissivity, σ is the Stephen Boltzmann constant, $X_{S_1S_2}$ is the angle coefficient of radiative heat transfer.

In the Cz-Si growth process, the radiative heat transfer is related to the crystal surface temperature and depends on the radiation and absorption effects of the solid surfaces. Figure 4a shows melt free surface temperature distributions, with the coordinate zero point being the triple point. According to the above analysis, as ΔR increases, the average melt temperature increases. The temperature on the melt free surface when ΔR = 35 mm is higher than that when ΔR = 15 mm, but when ΔR = 55 mm, the melt temperature near the triple point is lower than when ΔR = 15 mm. The heat shield can block the heat radiation from high-temperature solid parts and the melt free surface to the crystal. When ΔR = 55 mm, the jacket and the heat shield are far away from the crystal, making the radiative heat transfer area between the jacket and the melt free surface larger, thus enhancing the radiative heat transfer.

Figure 4b shows the heat flux distributions along the melt free surface. Near the triple point, the radiative heat transfer area of the melt free surface is enlarged as ΔR increases, which increases the heat flux. Near the crucible wall, the distance between the heat shield and the crucible decreases as ΔR increases, blocking the heat transfer at the melt surface and reducing the heat flux.

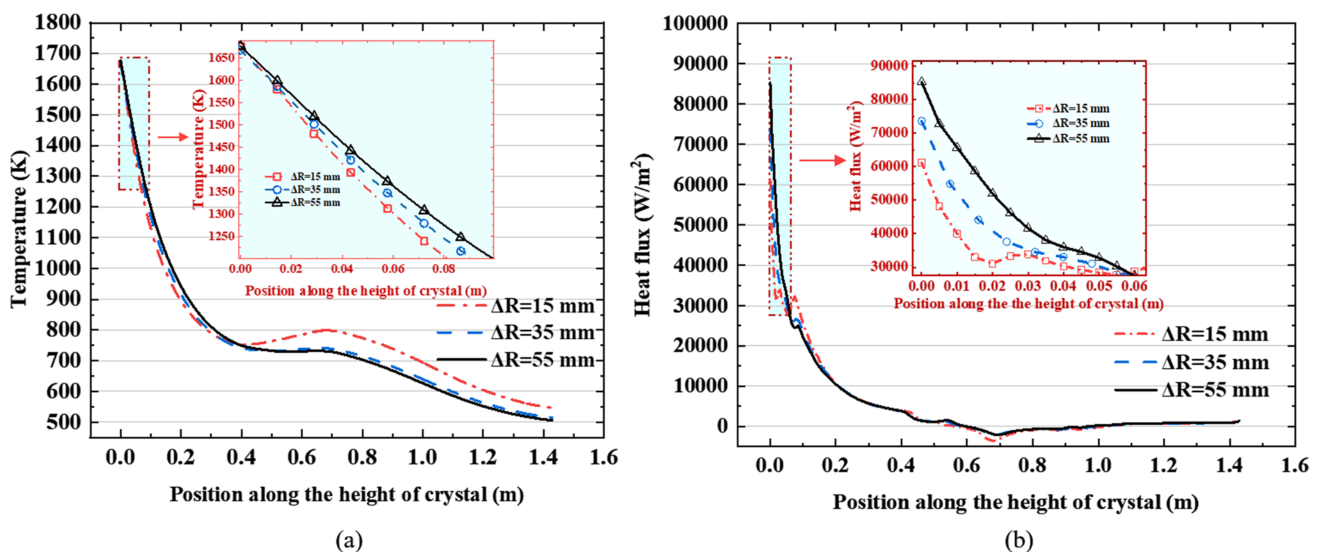

Fig. 5 **a** Temperature and **b** heat flux distributions along the crystal surface

The heat dissipation from the crystal surface affects the temperature distribution inside the crystal, thus affecting the crystal quality. Figure 5a shows the crystal surface temperature; the coordinate zero point is the triple point. It can be seen from the figure that, at the bottom of the crystal surrounded by the jacket (crystal height is 0 to 0.4 m), the crystal surface temperature gradually decreases as ΔR decreases indicating that the closer the jacket is to the crystal, the stronger the cooling effect at the crystal. Conversely, top of the crystal, the smaller the ΔR, the smaller the jacket's on the influence.

Figure 5b shows the heat flux along the crystal surface. According to Formula (9), the change in radiative heat transfer area on the crystal surface can be ignored; thus, the higher the temperature, the higher the radiative heat flux. For different ΔR, the crystal surface temperature difference near the triple point is small, but the difference in heat flux is more than 10,000 W/m^2.

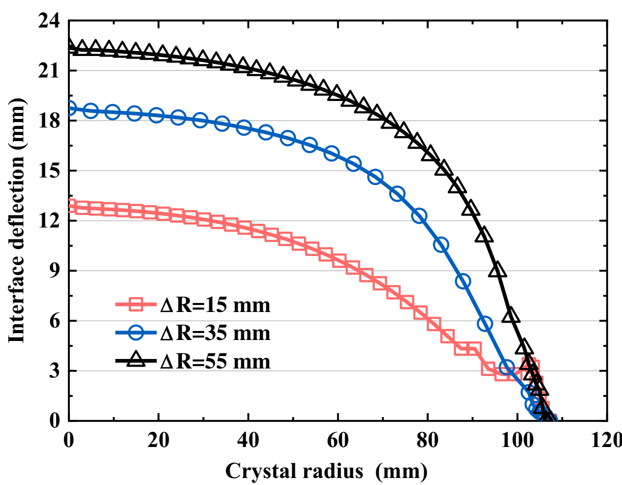

Fig. 6 S-L interface shape

3.4 Effect of water-cooling jacket on S-L interface shape and temperature gradient

A flat or slightly convex S-L interface shape can effectively avoid the occurrence of doping component segregation, micro defects, and dislocations. Figure 6 shows the comparison of S-L interface shapes; the height of the S-L interface increases by 10 mm. The crystal pulling rate is constant, the hot zone changes with the increase of the jacket radius, the cooling capacity of the jacket in the crystal is weakened, the latent crystallization heat is difficult to release, and the S-L interface moves upward. In other words, for ΔR = 15 mm, the S-L interface shape of ΔR = 55 mm can be reached when the crystal pulling rate is higher.

In addition, when the jacket is close to the crystal, the heat shield blocks the radiative heat transfer at the bottom of the crystal, but the argon flow rate increases. According to simulation results, the radiative heat flux is 8444.282 W/m^2, whereas the argon convection heat flux is 23936.148 W/m^2. Therefore, the cooling effect is mainly determined by the argon convection heat transfer at the bottom of the crystal.

The temperature gradient can affect the crystal growth rate and thermal stress. According to Formula (5), the crystal growth rate can be increased by raising the axial crystal temperature gradient and decreasing the melt axial temperature gradient. Figure 7a shows the axial temperature distributions; the coordinate zero point is the center point of the S-L

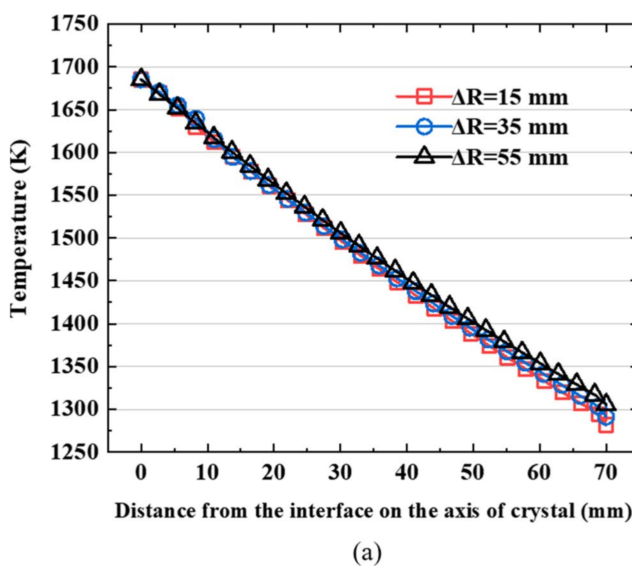

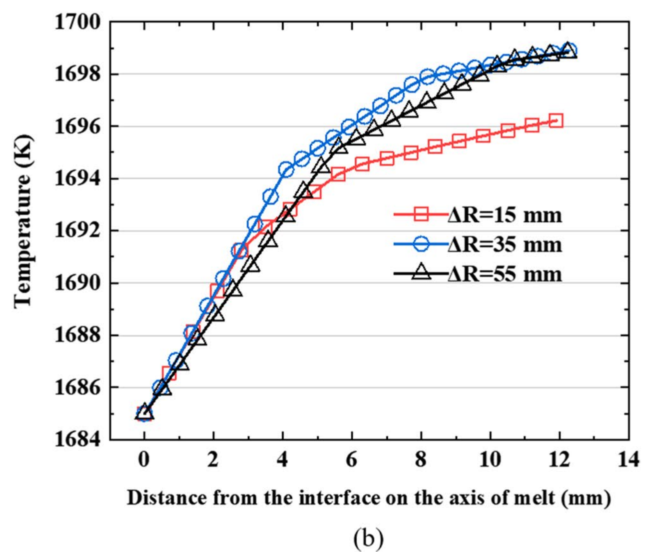

Fig. 7 Axial temperature distributions (**a**) crystal, (**b**) melt

interface. When ΔR = 15 mm, the crystal axial temperature difference is at its maximum. If the temperature gradient is too small, the heat cannot be exported in time, and constitutional undercooling at the S-L interface is likely to occur, affecting the normal crystal growth. When ΔR = 15 mm, 35 mm and 55 mm, the axial crystal temperature gradients are 5.76 K/mm, 5.62 K/mm and 5.42 K/mm, respectively. Reducing the jacket radius can increase the crystal axial temperature gradient.

The reduction of the melt axial temperature gradient can increase the crystal growth rate, reduce the power consumption of the heater, and weaken the silicon melt thermal convection. However, if the melt axial temperature gradient is too small, the melt at the S-L interface is prone to temperature fluctuations and component segregation, and the shape of the S-L interface will become unstable, even leading to the formation of new crystal nuclei. Figure 7b shows the melt axial temperature distributions. When ΔR = 15 mm, 35 mm, and 55 mm, the temperature gradient of the silicon melt is 0.94 K/mm, 1.16 K/mm, and 1.15 K/mm, respectively. When ΔR = 15 mm, the crystal axial temperature gradient is the largest and the melt is the smallest, which can improve the crystal growth rate. According to the calculation of the heat balance formula (Formula (5)), the crystal growth rate when ΔR = 15 mm is 27.1% and 36.1% higher than that when ΔR = 35 and 55 mm, respectively.

3.5 Effect of water-cooling jacket on thermal stress of crystal

The main reason for the thermal stress in the crystal is that the deformation of the S-L interface causes uneven thermal expansion. The thermal stress is positively linked to the temperature gradient in the crystal. Figure 8 shows the temperature distributions at the S-L interface near the triple point. The radial temperature gradient is minimal when ΔR = 15 mm and maximum when ΔR = 55 mm. The crystal temperature and thermal stress distributions

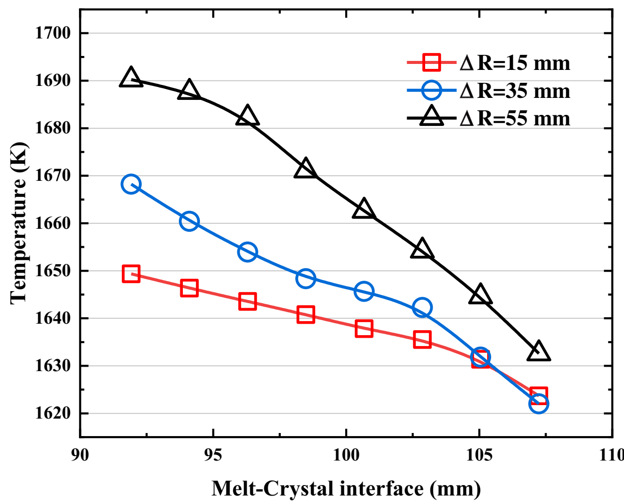

Fig. 8 Radial temperature distributions near the triple point

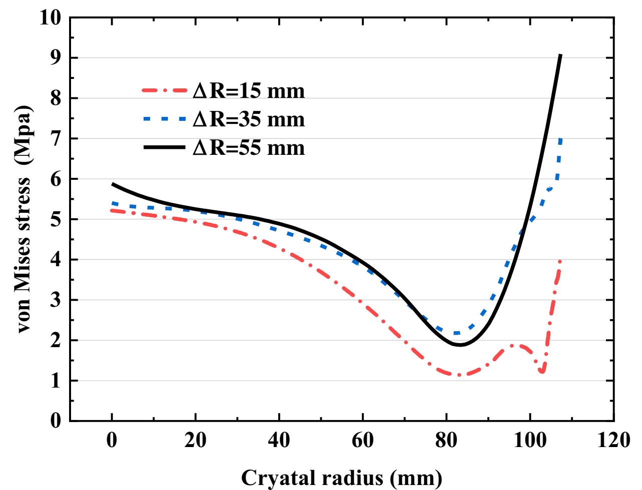

Fig. 10 Thermal stress distributions along the S-L interface

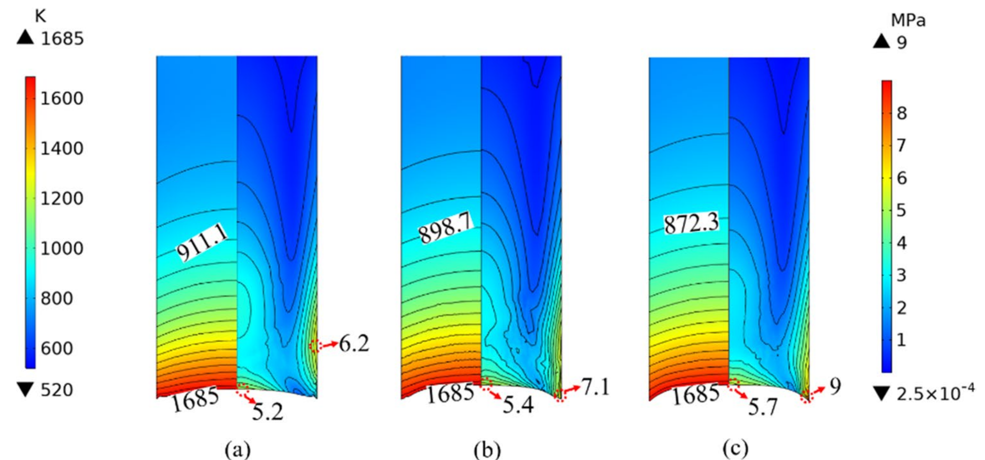

Fig. 9 Temperature and thermal stress distributions in the crystal (**a**)ΔR = 15 mm, (**b**) ΔR = 35 mm, (**c**)ΔR = 55 mm

are illustrated in Fig. 9. The thermal stress of the crystal increases as the increase of radial temperature gradient, and the thermal stress on the crystal surface is greater than that within the crystal. With respect to thermoelastic theory, the critical shear stress of the crystal at the S-L interface is very low. Figure 10 shows the thermal stress distributions of the S-L interface, and the thermal stress appears higher in the center or edge of the S-L interface. As is shown in Fig. 9c, when ΔR = 55 mm, the maximum thermal stress occurs to the edge, which is 9 MPa. Figure 9a shows that when ΔR = 15 mm, the maximum thermal stress occurs to the center, which is 5.2 MPa. At the same pulling rate, with ΔR decreases, the S-L interface is more flat, and the radial temperature gradient gets smaller, reducing the crystal compression stress and thermal stress. As the thermal stress is lower than the limit value, it is possible to increase the crystal pulling rate.

4 Conclusions

In this contribution, the influence of the change in radius of the water-cooling jacket on the growth of the Cz-Si crystal is studied numerically. By analyzing the temperature field and the flow field of the melt, the argon flux close to the heat shield, the shape of the S-L interface shape and the crystal thermal stress, it is concluded that:

(1). The change of radius of the water-cooling jacket has little effect on the silicon melt flow but has a significant effect on the heat transfer of the crystal. When the jacket radius decreases, although the radiative heat transfer at the crystal bottom is restrained, the argon flow rate near the crystal side wall increases significantly, which enhances the cooling effect in the crystal and reduces the convexity of the S-L interface.

(2). At the same pulling rate, when the radius of the water-cooling jacket decreases, the thermal stress in the crystal near the S-L interface decreases. According to the calculation results, when ΔR is reduced from 55 to 15 mm, the crystal growth rate can be increased by 36.1%, which can improve the production efficiency of Cz-Si while ensuring the crystal quality.

Authors' contributions Wenjia Su contributed to the conception of the study. Jiaqi Li and Jiulong Li performed the simulation and contributed significantly to analysis and manuscript written. Zhen Zhang performed the data analyses and modified the manuscript. Zhicheng Guan helped perform the analysis with constructive discussion.

Funding The Project is supported by Key Research and Development Program of Jiangsu Province of China (Grant No. BE2019009-003), Industry-University-Research Project (Wuxi Suntech Solar Power Co., Ltd. Grant No. 8421130025). The National Natural Science Foundation for Young Scholars of China (Grant No. 51206069).

Data Availability All data generated or analyzed during this study are included in this published article.

Code availability Not applicable.

The authors wish to acknowledge the financial support on this research from the Key Research and Development Program of Jiangsu Province of China (grant no. BE2019009-003), Industry–University Research Project (Wuxi Suntech Solar Power Co., Ltd., grant no. 8421130025), and the National Natural Science Foundation for Young Scholars of China (grant no. 51206069).

Declarations

Competing interests The authors declare no competing interests.

Conflict of interest There are no conflicts of interest.

Ethics approval Not applicable.

Consent to participate The consent was obtained from individual or guardian participants.

Consent for publication That all authors have checked the manuscript and have agreed to the submission.

References

1. Czochralski J (1918) Ein Verfahren zur Messung der Kristallisationsgeschwindigkeit der Metalle. Z Anal Chem 57(8):373–374. https://doi.org/10.1007/BF01473047
2. Uecker R (2014) The historical development of the Czochralski method. J Cryst Growth 401:7–24. https://doi.org/10.1016/j.jcrysgro.2013.11.095
3. Jeon H, Park H, Koyyada G et al (2020) Optimal Cooling System Design for Increasing the Crystal Growth Rate of Single-Crystal Silicon Ingots in the Czochralski Process Using the Crystal Growth Simulation. Processes 8:1077. https://doi.org/10.3390/pr8091077
4. Voronkov V (1982) The mechanism of swirl defects formation in silicon. J Cryst Growth 59(3):625–643. https://doi.org/10.1016/0022-0248(82)90386-4
5. Huang X, Taishi T, Wang T et al (2001) Measurement of temperature gradient in Czochralski silicon crystal growth. J Cryst Growth 229(1):6–10. https://doi.org/10.1016/S0022-0248(01)01040-5
6. Mukaiyama Y, Sueoka K, Maeda S et al (2020) Numerical analysis of effect of thermal stress depending on pulling rate on behavior of intrinsic point defects in large-diameter Si crystal grown by Czochralski method. J Crystal Growth 531:125334. https://doi.org/10.1016/j.jcrysgro.2019.125334
7. Tsukada T, Hozawa M, Imaishi N (1990) Effect of a radiation shield on thermal stress field during Czochralski crystal growth of silicon. J Chem Eng Jpn 23:186–191. https://doi.org/10.1252/jcej.23.186
8. Song D, Lee S, Mun H et al (2011) Oxygen content increasing mechanism in Czochralski (CZ) silicon crystals doped with heavy antimony under a double-typed heat shield. J Cryst Growth 325(1):27–31. https://doi.org/10.1016/j.jcrysgro.2011.04.020
9. Zhang J, Liu D, Zhao Y et al (2014) Impact of heat shield structure in the growth process of Czochralski silicon derived from

numerical simulation. Chin J Mechanic Eng 27(3):504–510. https://doi.org/10.3901/CJME.2014.03.504
10. Rojo C, Diéguez E, Derby J (1999) A heat shield to control thermal gradients, melt convection, and interface shape during shouldering in Czochralski oxide growth. J Cryst Growth 200(1):329–334. https://doi.org/10.1016/S0022-0248(98)01250-0
11. Prostomolotov A, Verezub N, Mezhennii M et al (2011) Thermal optimization of CZ bulk growth and wafer annealing for crystalline dislocation-free silicon. J Cryst Growth 318(1):187–192. https://doi.org/10.1016/j.jcrysgro.2010.11.080
12. Friedrich J, Jung T, Trempa M et al (2019) Considerations on the limitations of the growth rate during pulling of silicon crystals by the Czochralski technique for PV applications. J Crystal Growth 524:125168. https://doi.org/10.1016/j.jcrysgro.2019.125168
13. Sim B, Jung Y, Lee H (2009) Effect of the Ingot Cooling on the Grown-in Defects in Silicon Czochralski Growth. Jpn J Appl Phys 48(10R):105503. https://doi.org/10.1143/JJAP.48.105503
14. Zhao W, Liu L (2017) Control of heat transfer in continuous-feeding Czochralski-silicon crystal growth with a water-cooled jacket. J Cryst Growth 458:31–36. https://doi.org/10.1016/j.jcrysgro.2016.10.041
15. Qi X, Wang J, Wen Y et al (2023) Effect of water-cooled jacket on the oxygen transport during the Czochralski silicon crystal growth process. J Crystal Growth 609:127139. https://doi.org/10.1016/j.jcrysgro.2023.127139
16. Jung T, Seebeck J, Friedrich J (2013) Combined global 2D–local 3D modeling of the industrial Czochralski silicon crystal growth process. J Cryst Growth 368:72–80. https://doi.org/10.1016/j.jcrysgro.2013.01.026
17. Lan C (2004) Recent progress of crystal growth modeling and growth control. Chem Eng Sci 59(7):1437–1457. https://doi.org/10.1016/j.ces.2004.01.010
18. Qi X, Ma W, Dang Y et al (2020) Optimization of the melt/crystal interface shape and oxygen concentration during the Czochralski silicon crystal growth process using an artificial neural network and a genetic algorithm. J Crystal Growth 548:125828. https://doi.org/10.1016/j.jcrysgro.2020.125828

Publisher's Note Springer Nature remains neutral with regard to jurisdictional claims in published maps and institutional affiliations.

Springer Nature or its licensor (e.g. a society or other partner) holds exclusive rights to this article under a publishing agreement with the author(s) or other rightsholder(s); author self-archiving of the accepted manuscript version of this article is solely governed by the terms of such publishing agreement and applicable law.